Open Data Science to fight COVID-19: Winning the 500k XPRIZE Pandemic Response Challenge (Supplementary Material)

Miguel Angel Lozano[1], Òscar Garibo i Orts[2], Eloy Piñol[2], Miguel Rebollo[2], Kristina Polotskaya[3], Miguel Angel Garcia-March[2], J. Alberto Conejero[2], Francisco Escolano[1], and Nuria Oliver[4]

[1] University of Alicante, Alicante, Spain
malozano@ua.es
[2] IUMPA and VRAIN. Universitat Politècnica de València, València. Spain
[3] University Miguel Hernández, Elche, Spain
[4] ELLIS (European Lab. for Learning and Intelligent Systems) Unit Alicante, Spain

A Non-Pharmaceutical Interventions

Table 1 summarizes the NPIs considered in the Challenge, their meanings and possible levels of activation.

Table 1: NPIs considered in the Challenge. The predictor is trained with confinement interventions (C1 to C8). Both confinement and public health interventions are considered in the prescriptor.

NPI name	**Level 0**	**Level 1**	**Level 2**	**Level 3**	**Level 4**
Confinement Interventions					
C1. School closing	Nothing	Recommend closing	Partial closing (e.g. just high school, or just public schools)	Complete closing	
C2. Workplace closing	Nothing	Recommend closing (or work from home)	Require closing (or work from home) for some sectors/categories of workers	Require closing (or work from home) all-but-essential workplaces	
C3. Cancel public events	Nothing	Recommend cancelling	Require cancelling		
C4. Restrictions on gatherings	Nothing	Cancel very large gatherings (above 1000 people)	Cancel gatherings between 101-1000 people	Cancel gatherings between 11-100 people	Cancel gatherings of 10 or less people
C5. Close public transport	Nothing	Recommend closing (or significantly reduce volume, routes and/or means of transport available)	Require closing (or prohibit most citizens from using it)		

C6. Stay at home requirements	Nothing	Recommend not leaving home	Require not leaving house with exceptions for daily exercise, grocery shopping, and *essential* trips	Require not leaving house with minimal exceptions (e.g. allowed to leave once a week, or only one person can leave at a time, etc)	
C7. Restrictions on internal movement	Nothing	Recommend not to travel between regions/cities	Internal movement restrictions in place		
C8. International travel controls	Nothing	Screening arrivals	Quarantine arrivals from some or all regions	Banning on arrivals from some regions	

NPI name	**Level 0**	**Level 1**	**Level 2**	**Level 3**	**Level 4**
Public Health Interventions					
H1. Public information campaigns	No COVID-19 public information campaigns	Public officials urging caution about COVID-19	Coordinated public information campaign (e.g. across traditional and social media)		
H2. Testing policy	No testing policy	Only those who both (a) have symptoms AND (b) meet specific criteria (e.g. key workers, admitted to hospital, came into contact with a known case, returned from overseas)	Testing of anyone showing COVID-19 symptoms	Open public testing (e.g. "drive through" testing available to asymptomatic people)	
H3. Contact tracing	No contact tracing	Limited contact tracing; not done for all cases	Comprehensive contact tracing; done for all identified cases		
H6. Facial coverings	No policy	Recommended	Required in some specified shared/public spaces outside the home with other people present, or some situations when social distancing not possible	Required in all shared/public spaces outside the home with other people present or all situations when social distancing not possible	Required outside the home at all times regardless of location or presence of other people

B SIR Epidemiological Model

The predictors model the dynamics of the epidemics in each GEO j using a basic SIR compartmental meta-population model [1,2]. In this model, the population is divided into three different states: S (Susceptible), Z (Infected), and D (Removed, due to recovery or death). The dynamics of such an SIR model is given by the following set of differential equations:

$$\begin{aligned} \frac{dS^j}{dt} &= -\beta \frac{S^j}{P_j} Z^j \\ \frac{dZ^j}{dt} &= \beta \frac{S^j}{P_j} Z^j - \mu Z^j \\ \frac{dD^j}{dt} &= \mu Z^j \end{aligned} \tag{1}$$

where β is the infection rate which controls the probability of transition between the S and Z; and μ is the recovery or removal rate, controlling the probability of transition between the Z and D states. Previous work [9] has estimated $\mu = 0.08$ for SARS-CoV-2.

When discretizing $\frac{dZ^j}{dt}$ for two consecutive days, we get

$$Z_n^j = Z_{n-1}^j + \beta \frac{S_{n-1}^j}{P_j} Z_{n-1}^j - \mu Z_{n-1}^j = \left(1 + \beta \frac{S_{n-1}^j}{P_j} - \mu\right) Z_{n-1}^j. \tag{2}$$

which yields

$$R_n^j = \frac{(1-\mu)P_j}{S_n^j} + \beta = \frac{Z_n^j}{Z_{n-1}^j} \frac{P^j}{S_n^j}. \tag{3}$$

This equation is important as it establishes a relationship between the R_n^j and the parameters of the SIR model. The larger the R_n^j, the larger $\frac{Z_n^j}{Z_{n-1}^j}$ and hence the larger the growth in the number of cases. Given that μ is constant in Equation 3, the larger the infection rate β, the larger the R_n^j. Moreover, the infection rate and thus R_n^j depend on the applied NPIs.

In addition, if we predict the value $\hat{R}_n^j$, we can also predict the number of cases for day n at GEO j as

$$\widehat{X}_n^j = \left(\widehat{R}_n^j \frac{S_{n-1}^j}{P_j} - 1\right) K Z_{n-1}^j + X_{n-K}^j. \tag{4}$$

where K is the size of the temporal window (in days) used to compute the mean number of cases Z_n. As previously explained, in our case K = 7 days to mitigate the peculiarities in the reporting schedules of different GEOs and X_n and X_{n-k} are the reported new cases for days n and $n-k$, respectively; $\hat{R}_n$ is the predicted R_n; P_j is the population of GEO j; Z_{n-1}^j is the cumulative number of cases the averaged over K days for day $n-1$ and for GEO j.

The goal of the predictors is to estimate $\widehat{R}_n^j$ given the data up to day $n-1$, similarly as proposed in [7]. Given the dependency of R_n^j on the transmission rate and the dependency of the transmission rate on the NPIs, we describe next predictors that consider both the number of COVID-19 infections (*context*) and the applied NPIs (*actions*) in each GEO and for each day.

C Clustering of countries/regions

In order to build the bank of LSTMs, we clustered the regions using a K-means algorithm applied to the time series of reported number of cases per 100K inhabitants. We used the Elbow method to identify the optimal number of clusters (see Figure 1):

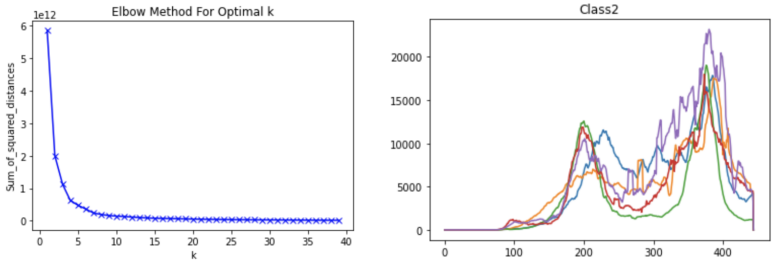

Fig. 1. Left: Selection of 15 clusters via K-means algorithm applied to the time series of reported number of COVID-19 cases. For 15 classes the total squared distance wrt the centers of the clusters is quite stable. Right: Example of one of the classes with the following GEOs: 'Colombia', 'Mexico', 'South Africa', 'Florida' and 'Texas'.

After optimizing the number of clusters, we obtained 15 different clusters (see t-SNE visualization in Figure 2). The Figures below illustrate the clustering of all the GEOs according to the temporal time series of their COVID-19 cases (Figure 3) and the allocation of each GEO to a model in the WT predictor (Figure 4).

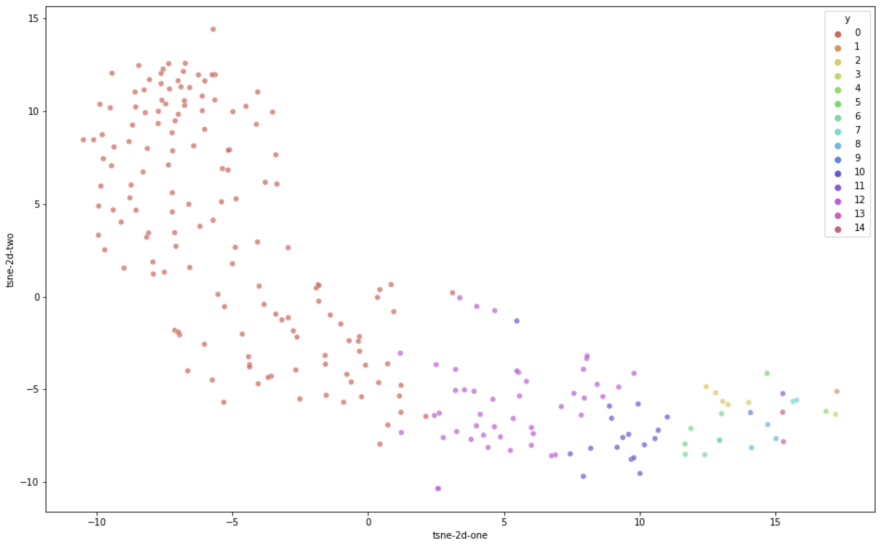

Fig. 2. Clusters and their spatial distribution in a t-SNE visualization.

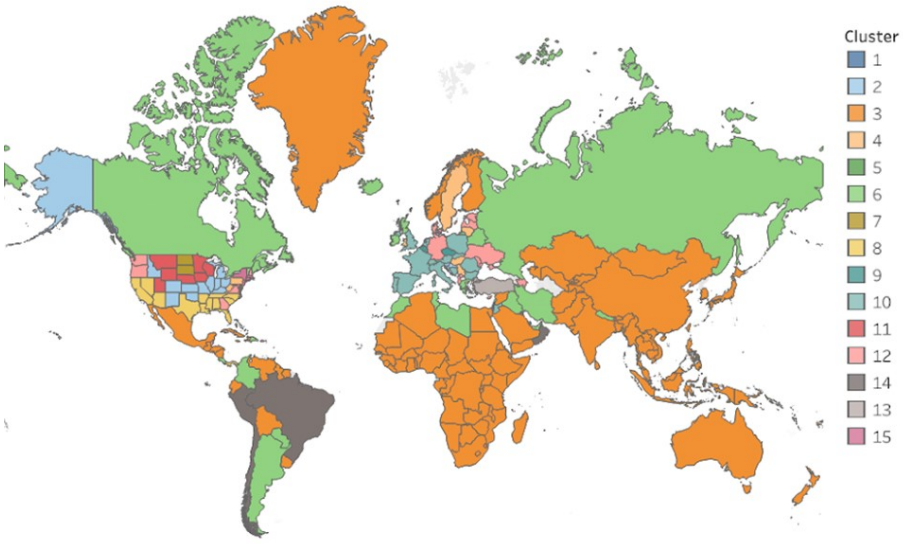

Fig. 3. Clusters obtained by optimizing a K-means algorithm applied to the time series of reported number of COVID-19 cases.

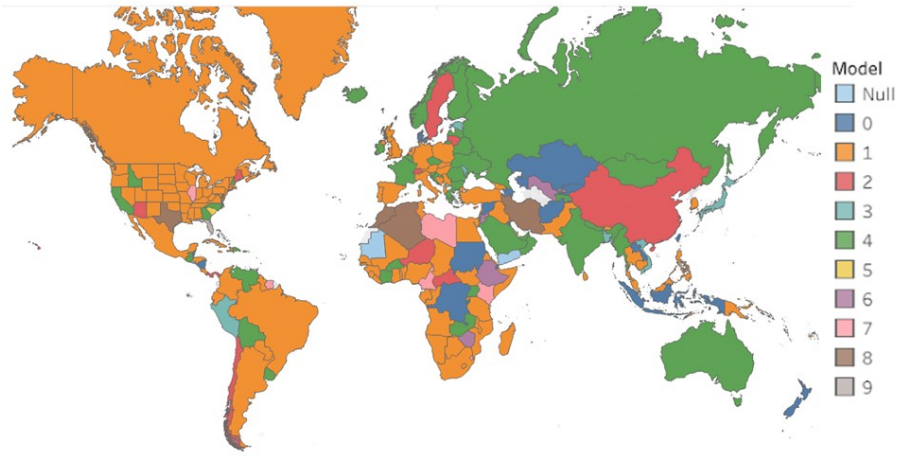

Fig. 4. WT Predictor model allocation, where numbers 0 and 1 correspond to the reference model, and numbers 2 to 9 correspond to the 8 different cluster models that we used in our bank. Note that null is the model we applied in Yemen and Mauritania, which assigns the number of cases based on statistics of the historic data instead of the machine-learning based prediction due to noise in the data.

D Convergence of R_n

D.1 Non-trivial long-term stationary states in epidemiological models

A stationary long-term state which is not the trivial state where all individuals are healthy occurs in several computational epidemiological models. For example, a non-trivial steady state is obtained in simple models derived as the individual mean-field limit of a system describing the spread of a disease in a network when cross-correlations are included (and hence non-linearities) [11,10,5]. Other examples are models obtained as the degree-based mean field limit of a system with house-hold structure [8,6], models that consider the age of the disease [4], etc. Let us detail the first example to motivate our discussion in next section.

Let us consider the spreading of a virus in a graph $G(D, L)$ with D nodes and L links. It is characterized by a symmetric adjacency matrix A. Nodes $\sigma_i(t)$ represent individuals. They can be in state $\sigma_i(t) = 1$ (infected) or $\sigma_i(t) = 0$ (healthy or cured). The infection process is given by a Poisson process with rate β . The recovery process is also a Poisson process, independent from the infection process, with rate γ. The state of the system at time t is thus $\sigma^s(t) = (\sigma_1(t), \sigma_2(t) \ldots, \sigma_D(t))$, and there are 2^D possible states, so $s = 0, \ldots, 2^D - 1$. Often it is called state of the system to $\sigma(t) = (\sigma^0(t) \ldots, \sigma^{2^D-1}(t))$. One can order these states in different ways. A conventional way is to order them as binary numbers (*e.g.*, for $D = 4$, $s = 0$ corresponds to 0000 or $s = 2$ corresponds to 0010). The number of states with c infected nodes is $\binom{D}{c}$.

The dynamics must consider the possible transitions between states $\sigma^s(t)$.

- Recovery dynamics: If individual i is infected, then the transition rate to cured is γ. Given the binary ordering described above, this means that the transition between state s where $\sigma_i(t) = 1$ and state s' where $\sigma_i(t) = 0$, is $q_{ss'} = \gamma$, with $s' = s - 2^{i_1-1}$. For state s this transition occurs for all nodes $\sigma_{i_1}(t)$ which are equal to 1 in state s. Then, here the transition rates $q_{ss'} = \gamma$.
- Contagion dynamics: If individual i is not infected, then it may be infected by all those individuals i' that are connected to it via the adjacency matrix (with elements $a_{ii'}$). The transition rates are β. Here the $s' = s + 2^{i_0+1}$, with i_0 running over all nodes which are in state 0 in state j. Here the transition rates $q_{ss'} = \beta \sum_{k=1}^{D} \sigma_k(t) a_{i_0 k}$. So node i_0 in state $\sigma^s(t)$ is connected via $a_{i_0 k}$ to the nodes with index k in current state. Those which are 1 may induce infection with rate β. Notice that in the sum all those which are in state 0 (i.e. not infected) do not contribute to the transition rate.

These are the transitions from state s to state s'. Then, in the Master equation these rates multiply the probability of being in state s'. Master equations, as balance equations, must include all transitions from any other state to state s. These multiply vector s so they can summed up into one coefficient. Therefore,

the Master equation reads

$$\frac{dP(\sigma^s(t))}{dt} = \sum_{s'=s-2^{i_1-1}} q_{ss'}P(\sigma^{s'}(t)) + \sum_{s'=s+2^{i_0-1}} q_{ss'}P(\sigma^{s'}(t)) - \sum_{k=0}^{2^{D-1}} q_{ks}P(\sigma^s(t)).$$

As a matrix, the generator with entries $q_{ss'}$ is a triangular matrix. In the diagonal one finds $q_{ss} = \sum_{k=0}^{2^{D-1}} q_{ks}$. For being a probability, one has to have that $\sum P(\sigma^s(t)) = 1$ as an additional condition.

To compute the probability of node i to be infected, we need to add all the probabilities corresponding to states with the node i equal to $\sigma_i(t) = 1$. That is $P(\sigma_i(t) = 1) = \sum_{s\in\{\bar{X}\}} \sigma^s(t)$, where $s \in \{\bar{X}_1\}$ means all those vectors with the condition that at node i they have a 1. Similarly, we proceed for it to be healthy (with $\sigma_i(t) = 0$), here $s \in \{\bar{X}_0\}$ which is the complementary set of $\{\bar{X}_1\}$. This resembles the expectation value of being at value σ_i, with $P(\sigma_i(t) = 1) + P(\sigma_i(t) = 0) = 1$. A quick way to relate the $P(\sigma^s(t))$ states with the $P(\sigma_i(t) = 1)$ is via the M matrix, whose rows are the states in binary representation (which the one we are using), so $P(\sigma_i(t) = 1) = P(\sigma^s(t))M$.

One can write down the generator of the evolution of only these two probabilities, $P(\sigma_i(t) = 1)$ and $P(\sigma_i(t) = 0)$. This is the matrix

$$Q_i = \begin{pmatrix} -q_{1i} & q_{1i} \\ q_{2i} & -q_{2i} \end{pmatrix}.$$

Here $q_{2i} = \gamma$ and $q_{1i} = \sum_{k=1}^{D} \beta a_{ik} 1_{\sigma_k(t)=1}$, with $1_{\sigma_k(t)=1} = 1$ if $\sigma_k(t) = 1$. To get to the mean field approximation one has to average the Master equation, which gives the equation for the $P(\sigma_i(t) = 1)$ as in the Glauber-Ising dynamics [3]. We call the averages $v_i(t) = P(\sigma_i(t) = 1)$ and the cross correlations $r_{ii'}(t) = P(\sigma_i(t) = 1|\sigma_{i'}(t) = 1)$. Then we get

$$\frac{dv_i(t))}{dt} = \beta \sum_{k=1}^{D} a_{ik} v_k(t) - \left(\beta \sum_{k=1}^{D} a_{ik} r_{ik}(t) + \gamma v_i(t) \right).$$

If we assume independence, i.e. $r_{ii'}(t)$ can be written as $r_{ii'}(t) = P(\sigma_i(t) = 1)P(\sigma_{i'}(t) = 1)$ then this gives a set of non linear equations:

$$\frac{dv_i(t))}{dt} = \beta \sum_{k=1}^{D} a_{ik} v_k(t) - \left(\beta \sum_{k=1}^{D} a_{ik} v_k(t) + \gamma \right) v_i(t).$$

The steady state is obtained by making the derivatives equal to zero at infinity (or for $D >> 1$) $\frac{dv_i(t))}{dt} = 0$. In this model there is a trivial solution in which at the steady state all individuals are healthy. But more importantly, there is a non-trivial solution where the probability of infection of a node at infinite time is non-zero. This solution is enabled by the non-linearity in the equations. This value is expressed $v_i(t \to \infty)) = v_{i,\infty}$. Indeed, as shown in [10], for any effective spreading rate $\tau = \beta/\gamma$ the non-zero steady state for the probability of

node i for being infected is can be expressed as the continued fraction

$$v_{i\infty} = \cfrac{1}{1+\tau d_i - \tau \sum_{j=1}^{D} \cfrac{a_{ij}}{1+\tau d_j - \tau \sum_{k=1}^{D} \cfrac{a_{jk}}{1+\tau d_k - \tau \sum_{q=1}^{D} \cfrac{a_{kq}}{1+\tau d_q - \ddots}}}},$$

with $d_i = \sum_{j=1}^{D} a_{ij}$ being the degree (the number of connections) of node i. We make two observations here: i) the stationary state is determined by the parameter τ and the adjacency matrix (which includes the statistics of the network). Note that when an NPI is applied, the network changes, as this is indeed the goal of the measure, *i.e.*, to ideally reduce the connections among individuals so as to minimize the community transmission of the disease. Then, the steady state is different for different NPIs when they are applied over sufficiently long periods of time; ii) The fact that the probability of infection is different from zero means that the total number of infected individuals increases steadily over time, and the number of susceptible individuals decreases.

D.2 Convergence of R_n

Let us briefly give some hints as to why the R_n, as defined in Eq. (3) in the paper, may be expected to converge to a number different than one. In the infinite time limit, the coefficient P^j/S^j_{n-1} is the inverse of the proportion of susceptible individuals in GEO j. According to the aforementioned discussion, this ratio will slightly change over time or be constant, while Z^j_n/Z^j_{n-1} would tend to one. Taking into account the existence of a non-zero steady state which depends on the NPI, as described in Section D, this would imply that R^j_n depends on the implemented NPI, impacting the time series of COVID-19 cases provided that the NPI is applied for long enough. Hence, for sufficiently long time periods, but not in the infinite time limit, we expect the system to reach an equilibrium point. As the system smoothly approaches the equilibrium, Z^j_n/Z^j_{n-1} may be slightly different from one. We conjecture that for large D, that is for large enough networks, all countries which are subject to the same NPI would end up with similar networks. Thus, in the infinite and long-time limits, we would expect a convergence to the same R_n and therefore the convergence behavior would not be an artifact of the predictor but would correspond to an underlying real-world phenomenon. This scaling property, requires a detailed proof that is part of our future work.

E Modeling the NPI-$\hat{R}_n$ space

Figure 5 (left) depicts the histogram of all possible NPI combinations for each value of stringency with unitary costs. Figure 5 (right) shows the number of combinations for which we computed the convergence R_n.

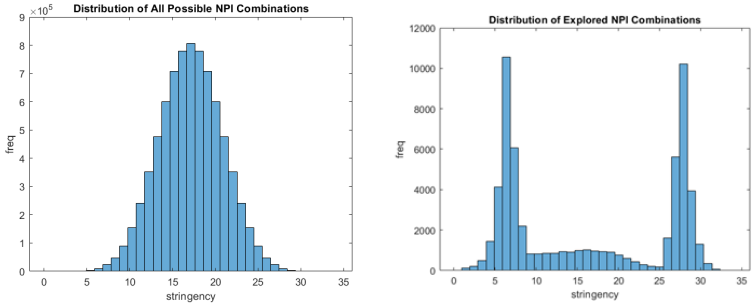

Fig. 5. Left: Histogram of all possible NPI combinations arranged by stringency at unitary costs. Right: Histogram of NPI combinations for which we obtained the NPI-R_n mapping, by stringency.

Figure 6 shows the feature importance analysis of the 12 different NPIs according to Gradient Boosted Trees.

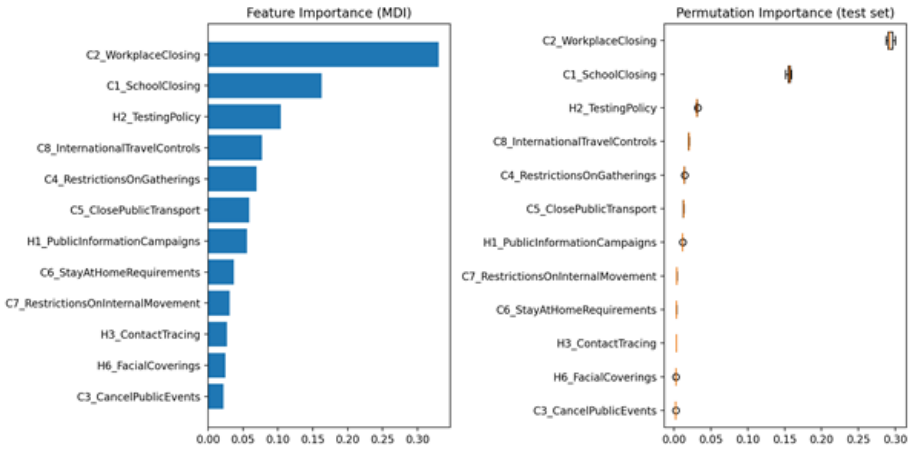

Fig. 6. Feature importance analysis of the NPIs using Gradient Boosted Trees.

F Prescriptor implementation

F.1 Obtaining the Pareto front

Given the input cost vector for a given GEO j ($Cost^j$), and our NPI-$\hat{R}_n$ matrix M, the Pareto front of j is computed at runtime as follows:
1. Apply the input costs to obtain the **stringency** for each NPI combination.
2. Obtain a **feature importance-weighted stringency** vector given by the $Cost^j$ divided by the feature importance of each dimension of the NPI vector.
3. Select a cost column $M_{,cost}$ (the cost may be stringency or feature importance-weighted stringency) and incidence column $M_{,inc}$ (given by the convergence $\hat{R}_n$ or total estimated COVID-19 cases in 20 or 60 days).
4. Sort the matrix of NPIs by $M_{,cost}$ in first place, and $M_{,inc}$ in second place.
5. Create an empty set of selected NPIs in the Pareto front ($selected = \{\}$)
6. For each row i in M, if $M_{i,inc}$ is lower than incidence of the last selected NPI, then add M_i to the *selected* set.

We select the NPIs that are at the intersection of the sets obtained considering both convergence $\hat{R}_n$ and total cases in 20 or 60 days, and stringency and feature importance-weighted stringency as cost and incidence columns respectively.

Figure 7 shows an example visualization of the Pareto front of the NPIs at unitary costs. The color of each dot represents the area in the (cases, stringency)-space of each NPI vector, with the cases normalized as follows

$$cases_N = \frac{cases - \min cases}{\max cases - \min cases}$$

F.2 Selection of NPIs from the Pareto front

Once we have a set of candidates in the Pareto front, the prescriptor selects a maximum of 10 recommended NPIs. In order to keep the most promising NPI combinations, each NPI is assigned a score, obtained as follows. First, the NPI combinations are sorted by cost; next, given the coordinates of NPI i, $c_i = (M_{i,cost}, M_{i,inc})$, the score for NPI i, $score_i$ is computed as:

$$score_i = 1 - \frac{angle(c_{i+1} - c_i, c_{i-1} - c_i) - \frac{\pi}{2}}{\pi}$$

That is, the maximum score is obtained when the angle that forms the NPI vector to the next point wrt the vector of the previous point in the Pareto front is close to $\frac{\pi}{2}$. Conversely, this score is minimum when this angle is close to $\frac{3\pi}{2}$.

All the NPIs whose score is not maximum within a local window in the cost axis are discarded.

F.3 Dynamic Intervention Policy selection

Finally, the prescriptor needs to provide an Intervention Policy, *i.e.* a *dynamic* regime of applying the selected NPIs over the time period of interest. To do

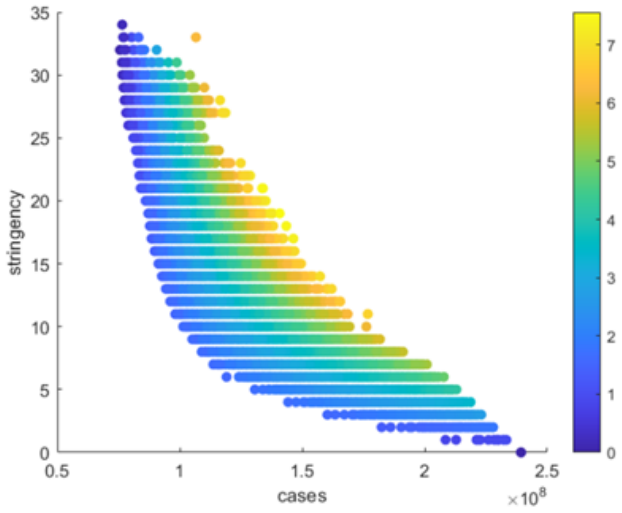

Fig. 7. Exemplary visualization of the Pareto front of NPIs with their associated stringencies at unitary costs.

so, we compute all possible combinations of subsequently applying the selected NPIs in chunks of minimum 14 days (to enable the NPIs to act) and identify the Pareto-front set of combinations that would yield the optimal trade-off between stringency and number of cases. The total number of chunks is dynamically determined, depending on the length of the time period of interest.

Figure 8 depicts an example of such a Pareto front, computed from an initial set of 19 candidate NPIs, *i.e.* the NPIs that are on the Pareto front as per the analysis previously described. In the Figure, the system defines temporal chunks of at least 21 days before changing NPIs and computes the NPI dynamic policy for a period of 60 days. There are 6,859 possible dynamic regimes of applying the NPIs. Of those, 225 (marked in red in the Figure) dominate the rest and constitute a Pareto front of the dynamic NPI policy selection. The color of each dot represents the area in the (cases, stringency)-space of such dynamic NPI combination, normalizing the number of cases as in Figure 7.

From such the set of Intervention Policies on the Pareto front, the prescriptor selects the 10 prescriptions that (1) are not dominated by any other policy; (2) contribute to having a diverse set of policies along the stringency axis and (3) minimize the changes in NPIs, as every NPI change has a social cost from a practical perspective.

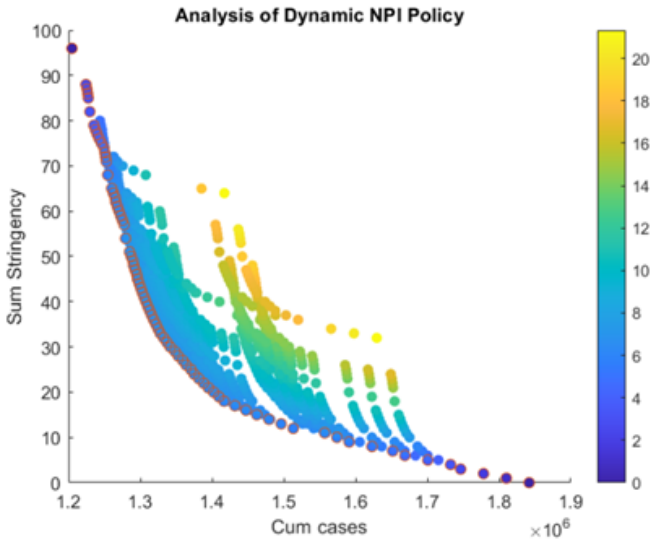

Fig. 8. Exemple of dynamic Intervention Policy optimization: from 6,859 possible Intervention Policies, 225 are on the Pareto front.

G Prescriptor visualization

Given that the main users of our prescriptor are non-experts (policy-makers, business owners or even citizens), we developed a visualization tool to communicate the ten Intervention Policies (IP) recommended for each GEO and to enable the comparison between two IPs.

The Figures below show a screen shot of the two interfaces of our visualization tool, which can be found here[5].

[5] https://public.tableau.com/app/profile/kristina.p8284/viz/PrescriptionsWeb/Visualize

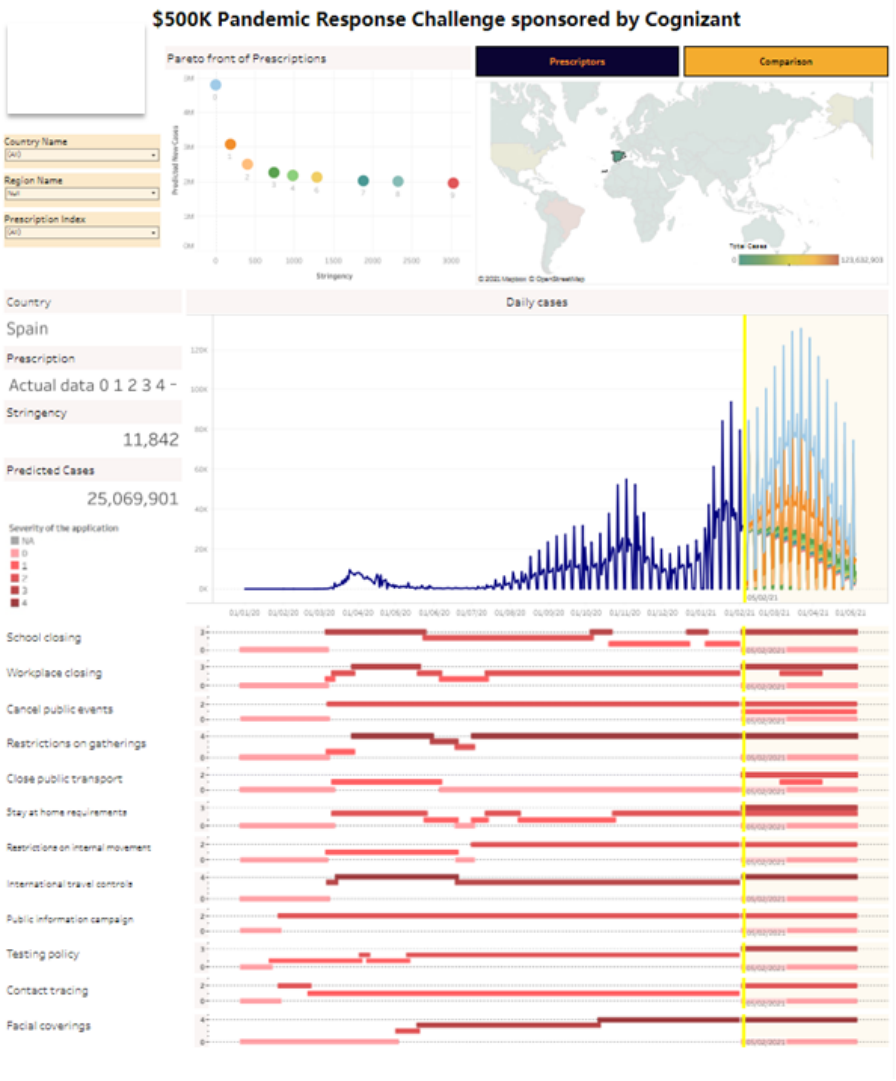

Fig. 9. Main window of the visualization tool for the prescriptor. It enables users to select the country/region of interest before it shows the 10 recommended prescriptions with their associated stringencies, total number of predicted COVID-19 cases and levels of activation of each of the 12 dimensions of the NPI vector. It also shows the Pareto front of all prescriptions. In this example, the system shows the 10 selected prescriptions for Spain.

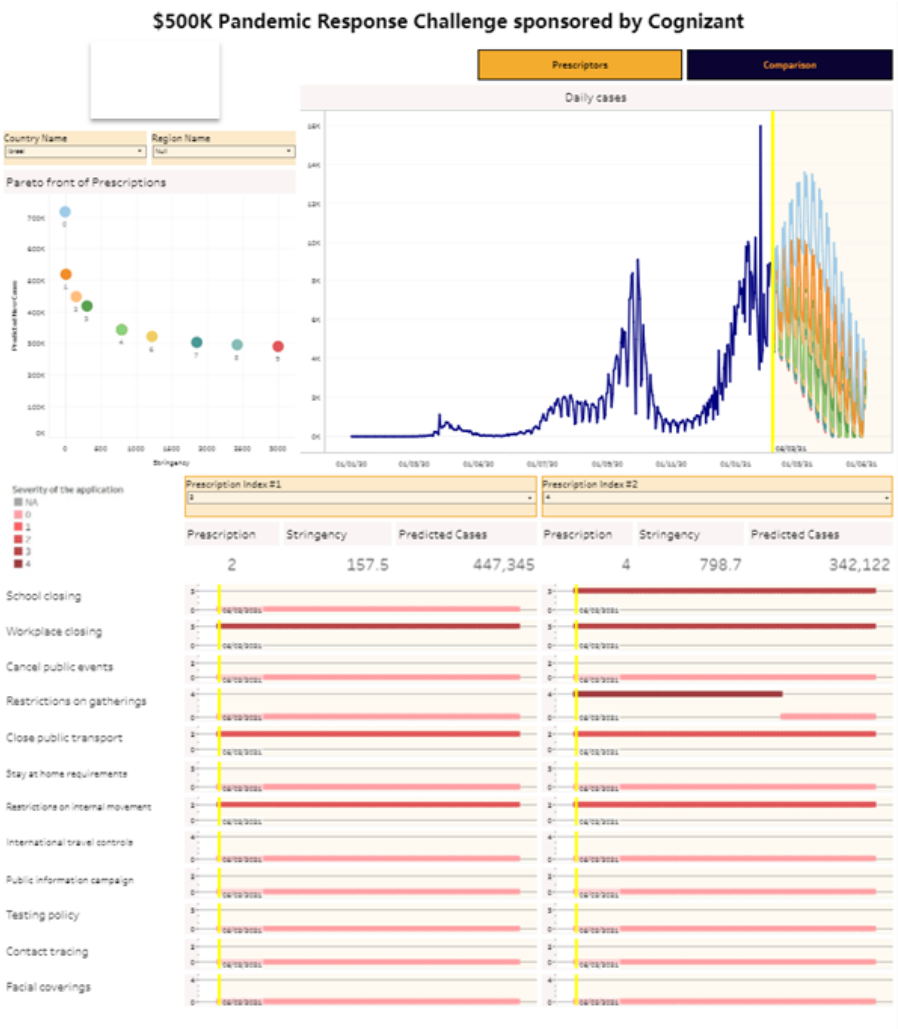

Fig. 10. Secondary window of the visualization tool called "Compare prescriptions". It enables users to select 2 prescriptions of Intervention Policies to compare. In this example, the system shows side to side two prescriptions from the 10 prescriptions proposed for Israel. The prescription on the left (#2) has an overall stringency of 157.5 and would result in 447,345 cases. The prescription on the right (#4) has an overall stringency of 798.7 and would result in 342,122 cases.

References

1. Allen, L.: Some discrete-time SI, SIR, and SIS epidemic models. Math. Biosci. **124**(1), 83–105 (1994)
2. Brauer, F., Driessche, P.d., Wu, J.: Lecture notes in mathematical epidemiology. Berlin, Germany. Springer **75**(1), 3–22 (2008)
3. Glauber, R.: Time-dependent statistics of the Ising model. J. Math. Phys. **4**(2), 294–307 (1963)
4. Inaba, H.: Age-structured population dynamics in demography and epidemiology. Springer (2017)
5. Kiss, I., Miller, J., Simon, P., et al.: Mathematics of epidemics on networks: From exact to approximate models, Interdisciplinary Applied Mathematics, vol. 46. Springer (2017)
6. Liu, J., Wu, J., Yang, Z.: The spread of infectious disease on complex networks with household-structure. Physica A: Statistical Mechanics and its Applications **341**, 273–280 (2004)
7. Miikkulainen, R., Francon, O., Meyerson, E., Qiu, X., *et al.*: From prediction to prescription: Evolutionary optimization of nonpharmaceutical interventions in the COVID-19 pandemic. IEEE Trans. Evol. Comput. **25**(2), 386–401 (2021)
8. Moreno, Y., Pastor-Satorras, R., Vespignani, A.: Epidemic outbreaks in complex heterogeneous networks. Eur. Phys. J. B **26**(4), 521–529 (2002)
9. Rojas, S.: Comment on "estimation of COVID-19 dynamics "on a back-of-envelope": Does the simplest SIR model provide quantitative parameters and predictions?". Chaos, Solitons & Fractals: X **5**, 100047 (2020)
10. Van Mieghem, P., Omic, J., Kooij, R.: Virus spread in networks. IEEE/ACM Trans. Netw. **17**(1), 1–14 (2008)
11. Wang, Y., Chakrabarti, D., Wang, C., Faloutsos, C.: Epidemic spreading in real networks: An eigenvalue viewpoint. In: 22nd International Symposium on Reliable Distributed Systems, 2003. Proceedings. pp. 25–34. IEEE (2003)